LAUNCH VEHICLE ASCENT TRAJECTORY DESIGN FOR OPTIMIZING ORBIT INJECTION CONDITIONS

Abel de Lima Nepomuceno, **mailto:abel@iae.cta.br**
Instituto de Aeronáutica e Espaço, Pça. Eduardo Gomes, 50, CEP 12228-904, São José dos Campos – SP; Brasil

Sandro da Silva Fernandes, **mailto:sandro@ief.ita.br**
Instituto Tecnológico de Aeronáutica, Pça. Eduardo Gomes, 50, CEP 12228-900, São José dos Campos – SP; Brasil

Abstract. *It is presented a proposition concerning ascent trajectory design for launch vehicles, aiming optimization of orbit injection conditions. The contextual considerations of launch mission, and corresponding development which lead to the settlement of required conditions, are included. In order to theoretically support the development in this work, and focusing the necessary for such, some Calculus of Variations concepts are disclosed. Then, a model has been developed with support on gradient-type method. To attain an effective serviceable product, diverse pertinent issues have been addressed, including convergence, a relevant issue in iterative optimization methods. Based on the aforementioned developed model, a software prototype has been implemented, as to allow the assessment of the model. The tests have been run within an already available and certified software which simulates the dynamics and flight attributions of a target launch vehicle. This simulation arrangement provides appropriate conditions for a fair assessment of the trajectory design model. Presenting collected results from simulation tests, it can be verified the good performance of the developed model. It could provide successful orbit injection, even in face of divergences from expected values on flight parameters. The software prototype has been implemented so that it can be used in the fashion of preflight trajectory design application, as well as in the fashion of an onboard guidance task.*

Keywords*: launch vehicles, trajectory optimization, flight mechanics*

1. INTRODUCTION

The considered launch vehicle is configured with solid-propellant stages. Hence, once burning starts in each stage, it proceeds without interruption for a fixed time interval, till final burnout, providing a thrust whose variable magnitude is prescribed. In the ascent stage, control over the vehicle is done through thrust direction, which is accomplished by means of movable nozzles. The last, deploy stage, is meant for complementing kinetic conditions for orbit injection, with fixed direction thrust. Thus, the satellite final orbit is already determined at the starting instant of the deploy stage, when the vehicle should be stabilized in a determined longitudinal attitude, so that it can achieve, with the complementation provided by last stage, the appropriate velocity for orbit injection.

Flight is ballistic between end of the previous ascent and start of the deploy stage, beyond atmosphere. During this phase, a pointing algorithm (Leite Filho and Pinto, 1998) evaluates ongoing flight conditions and determines what should be that longitudinal attitude for the deploy stage, as well the ignition instant of the stage, for the possible satellite orbit. Then the vehicle is put in the calculated attitude, without interference in its Keplerian trajectory. Since this trajectory is Keplerian, that ongoing flight conditions evaluated by the pointing algorithm are already settled at the beginning of the trajectory, that is, at the end of the ascent stage. So, for a desired satellite orbit, the vehicle must reach certain conditions at the end of this ascent stage.

This work presents a model for the ascent trajectory design, stressing the fulfillment of its required final conditions. The model is developed in a basis of Calculus of Variations, taking a gradient-type method as optimization method.

2. THEORETICAL BASIS

2.1. The optimal control problem

Let be considered a dynamic system with fixed initial state, fixed initial and final instants, and unbounded state and control spaces. The system state is made up of the *n*–vector of state variables $\mathbf{x}(t) = (x_1(t) \ \cdots \ x_n(t))^T \in R^n$, and the system control is made up of the *m*–vector of control variables $\mathbf{u}(t) = (u_1(t) \ \cdots \ u_m(t))^T \in R^m$. The following set of state differential equations define the system dynamics:

$$\dot{\mathbf{x}} = \mathbf{f}(\mathbf{x}, \mathbf{u}) \tag{1}$$

where $\mathbf{f} : R^n \times R^m \to R^n$. It is assumed that functions $f_i(.)$ and their partial derivatives $\partial f_i / \partial x_j$, $i, j = 1, ..., n$, are defined and continuous on $R^n \times R^m$. Let be considered a given time interval $[t_0, t_f]$, and a given initial state:

$$\mathbf{x}(t_0) = \mathbf{x}_0 \tag{2}$$

The control problem under consideration has the requirement of achieving some final state $\mathbf{x}(t_f)$, such that the following q ($q \leq n$) final equality conditions are satisfied:

$$\boldsymbol{\Psi}(\mathbf{x}(t_f)) = \begin{pmatrix} \Psi_1(\mathbf{x}(t_f)) & \cdots & \Psi_q(\mathbf{x}(t_f)) \end{pmatrix}^T = \mathbf{0} \tag{3}$$

where $\boldsymbol{\Psi} : R^n \to R^q$. It is assumed that functions $\Psi_k(.)$ and their partial derivatives $\partial\Psi_k/\partial x_j$, $k = 1, \ldots, q$, $j = 1, ..., n$, are defined and continuous on R^n. Besides the fulfillment of the above required equality conditions, it is established an optimization criterion (Bryson Jr. and Ho, 1975) for the phase trajectory over the time interval $[t_0, t_f]$ and for the final state at t_f, which is to minimize the performance index:

$$PI = K_G G(\mathbf{x}(t_f)) + K_L \int_{t_0}^{t_f} L(\mathbf{x}(t), \mathbf{u}(t)) dt \tag{4}$$

where $G : R^n \to R$ and $L : R^n \times R^m \to R$. It is assumed that functions $G(.)$, $L(.)$, and partial derivatives $\partial G/\partial x_i$, $\partial L/\partial x_i$, $i = 1, ..., n$, are continuous. K_G and K_L are positive weighting parameters.

The optimization problem is to determine an optimal control $\mathbf{u}^*(t)$ for $t \in [t_0, t_f]$, capable of transferring the system, by means of the dynamics in Eq. (1), from initial state at t_0 (Eq. (2)), to a final state at t_f so that final conditions (Eq. (3)) are satisfied, and minimizing the performance index Eq. (4). The corresponding phase trajectory is denoted optimal trajectory, $\mathbf{x}^*(t)$. This variational problem with such performance index Eq. (4) is called a Bolza problem. When the index does not contain component function on boundary values like the above function G, but only the integral component, the problem is called a Lagrange problem. When the index does not contain integral component like the above with function L, but only function on boundary values, the problem is called a Mayer problem (McIntyre, 1968).

2.2. Variational problem transformations

The foregoing Bolza problem may be transformed into a Mayer problem, by defining an auxiliary state variable x_{n+1} so that $\dot{x}_{n+1} = f_{n+1}(\mathbf{x}, \mathbf{u}) = L(\mathbf{x}, \mathbf{u})$, with $x_{n+1}(t_0) = 0$; thus yielding $K_G G(\mathbf{x}(t_f)) + K_L x_{n+1}(t_f)$ as the performance index to minimize, which configures a Mayer problem. The following definitions for the n+1 state equations and n+1 initial conditions incorporate the new auxiliary state variable x_{n+1}.

$$\dot{\bar{\mathbf{x}}} = \bar{\mathbf{f}}(\bar{\mathbf{x}}, \mathbf{u}) \tag{5}$$

$$\bar{\mathbf{x}}(t_0) = \bar{\mathbf{x}}_0 \tag{6}$$

Also, depending upon the numerical method chosen to solve the problem, it may be worthwhile to get hid of final conditions as formulated in Eq. (3), by incorporating them into the performance index, regarding that, in the numerical solution process, such final conditions are to be satisfied to some precision level. Introducing the q positive weighting parameters $K_{\Psi 1}$, …, $K_{\Psi q}$, the new performance index to minimize becomes:

$$\Phi(\bar{\mathbf{x}}(t_f)) = K_G G(\mathbf{x}(t_f)) + K_L x_{n+1}(t_f) + \sum_{k=1}^{q} \left(K_{\Psi k} \left(\Psi_k(\mathbf{x}(t_f)) \right)^2 \right) \tag{7}$$

Now, the equivalent optimization problem is enunciated as to determine an optimal control $\mathbf{u}^*(t)$ for $t \in [t_0, t_f]$, capable of transferring the system, by means of the dynamics in Eq. (5), from initial state at t_0 (Eq. (6)), to a final state at t_f, in such a way to minimize the performance index Eq. (7).

2.3. Gradient method

This also called steepest descent method (McIntyre, 1968) is used in this work to solve the above specified optimal control problem. Introducing the adjoint (n+1)-vector $\bar{\boldsymbol{\lambda}}(t) = \begin{pmatrix} \lambda_1(t) & \cdots & \lambda_n(t) & \lambda_{n+1}(t) \end{pmatrix}^T \in R^{n+1}$ of Lagrange multipliers for the constraints in Eq. (5), and the Hamiltonian function $H(\bar{\mathbf{x}}, \bar{\boldsymbol{\lambda}}, \mathbf{u}) = \bar{\boldsymbol{\lambda}}^T \bar{\mathbf{f}}(\bar{\mathbf{x}}, \mathbf{u})$, we form the augmented performance index:

$$J = \Phi + \int_{t_0}^{t_f} \bar{\boldsymbol{\lambda}}^T \left(\dot{\bar{\mathbf{x}}} - \bar{\mathbf{f}} \right) dt = \Phi + \int_{t_0}^{t_f} \left(\bar{\boldsymbol{\lambda}}^T \dot{\bar{\mathbf{x}}} - H \right) dt \tag{8}$$

In Eq. (8), since $(\dot{\bar{\mathbf{x}}} - \bar{\mathbf{f}})$ is null, minimizing J is equivalent to minimizing Φ. As necessary conditions for optimality, the adjoint vector $\bar{\boldsymbol{\lambda}}$ must satisfy the following adjoint differential equations, known as Euler-Lagrange equations, and final transversality conditions, respectively:

$$\dot{\bar{\boldsymbol{\lambda}}}(t) = -H_{\bar{\mathbf{x}}}^T \tag{9}$$

$$\bar{\boldsymbol{\lambda}}(t_f) = -\Phi_{\bar{\mathbf{x}}(t_f)}^T \tag{10}$$

Partial derivatives, $\Phi_{\bar{\mathbf{x}}}, H_{\bar{\mathbf{x}}}, H_{\mathbf{u}}$, are considered row vectors. Let $\mathbf{u}^0(t)$ be a initial estimate for control driving the system from the given initial state at t_0 to a final state at t_f, but producing a non-optimal value $J(\mathbf{u}^0)$ for the performance index. Expanding Eq. (8) in Taylor series about $J(\mathbf{u}^0)$, and truncating after the first order terms, leads to:

$$\delta J = \left(\Phi_{\bar{\mathbf{x}}} + \bar{\boldsymbol{\lambda}}^T\right)_{t=t_f} \delta\bar{\mathbf{x}}(t_f) - \int_{t_0}^{t_f} \left[\left(H_{\bar{\mathbf{x}}} + \bar{\boldsymbol{\lambda}}^T\right)\delta\bar{\mathbf{x}} + H_{\mathbf{u}}\delta\mathbf{u}\right] dt \tag{11}$$

Using Eqs. (9) and (10) on Eq. (11), yelds:

$$\delta J = -\int_{t_0}^{t_f} H_{\mathbf{u}}\delta\mathbf{u}\, dt \tag{12}$$

Now, as $J(\mathbf{u}^0)$ is not minimal, we can achieve a minor value $J(\mathbf{u}^1) = J(\mathbf{u}^0) + \delta J$ with a negative δJ, by means of appropriate $\delta\mathbf{u}(t)$, $t_0 \le t \le t_f$. So, to minimize J, we minimize δJ (steepest descent). But, we are limited by the linearity assumption in the Taylor series expansion and truncation; so we restrict $\delta\mathbf{u}(t)$, requiring that:

$$\int_{t_0}^{t_f} \delta\mathbf{u}^2 dt = K^2 \tag{13}$$

where K is some small positive quantity, chosen to quantify the step in control correction. Hence, we have the optimization problem of minimizing δJ, Eq. (12), subject to the constraint on $\delta\mathbf{u}(t)$, Eq. (13). In Calculus of Variations, this problem is configured as a isoperimetric problem (Golfetto, 2004), whose solution is:

$$\delta\mathbf{u} = K\left(\int_{t_0}^{t_f} H_{\mathbf{u}}^2 dt\right)^{-1/2} H_{\mathbf{u}}^T \tag{14}$$

From Eqs. (12) and (14), the corresponding change in performance index is $\delta J = -K\left(\int_{t_0}^{t_f} H_{\mathbf{u}}^2 dt\right)^{1/2}$.

The process to find a solution is iterative; the value of parameter K may be refined from any iteration to the next, as consequence of some convergence evaluation. A computational procedure for the method is as follows:

step 0) Establish and record a initial estimate $\mathbf{u}^0(t)$, $t_0 \le t \le t_f$, for the control.

step 1) Starting with initial state in Eq. (6), integrate the system state from t_0 to t_f, using Eq. (5) within the effective control. Record the phase trajectory $\bar{\mathbf{x}}(t)$.

step 2) Equation (3) may be computed at this point. If the final equality constraints are satisfied, and this is the only issue that really matters, the process may be finished at this point, with currently effective control being the solution.

step 3) With Eq. (10), compute the final values $\bar{\boldsymbol{\lambda}}(t_f)$. Starting with these values, integrate backward, from t_f to t_0, the adjoint equations using Eq. (9), and the non-negative integrand $H_{\mathbf{u}}^2$, to obtain $\int_{t_0}^{t_f} H_{\mathbf{u}}^2 dt$. Record $H_{\mathbf{u}}(t)$.

step 4) If $\int_{t_0}^{t_f} H_{\mathbf{u}}^2 dt \cong 0$, to the desired precision level, the minimal J has been reached, the currently effective control is the solution and the process is finished. Yet, some other criteria may be used to finish or not the process.

step 5) Using Eq. (14) with recorded $H_{\mathbf{u}}(t)$, compute $\delta\mathbf{u}(t)$, and add it to the effective control, getting a new control estimate for a new iteration, restarting from step 1.

3. TRAJECTORY DESIGN

3.1. Satellite deploy requirements

The launch mission is to deploy a satellite in terrestrial circular orbit of radius R_{SP}; hence its velocity must be orthogonal to its geocentric positional radius and have the magnitude $V_{SP} = (\mu/R_{SP})^{1/2}$, where μ=398601,2 Km^3/s^2.

The pointing algorithm (Leite Filho and Pinto, 1998) uses an impulsive model, also used here, for the burning in deploy stage: the nominal orbital velocity $\boldsymbol{V}_{SP}$ at the injection point results from the vector addition $\boldsymbol{V}_D+\boldsymbol{\delta V}_D$, where $\boldsymbol{V}_D$ is the velocity at the end of ballistic phase and $\boldsymbol{\delta V}_D$ is the increment provided by the burning of deploy stage. In our case, the orbital plane is the same as the flight plane, defined by vehicle geocentric distance and velocity vectors of ballistic phase prior to deploy stage, that is, $\boldsymbol{V}_D$, $\boldsymbol{\delta V}_D$ and $\boldsymbol{V}_{SP}$ are coplanar on that plane. β_D is the trajectory angle; θ_D is the pointing angle. Circumferential and radial components of the above vector addition should be:

$$V_D \cos\beta_D + \delta V_D \cos\theta_D = V_{SP} = (\mu/R_{SP})^{1/2} \tag{15}$$

$$V_D \sin\beta_D + \delta V_D \sin\theta_D = 0 \tag{16}$$

With the purpose of suppressing θ_D, yet assuring both above conditions keep holding, we get:

$$V_D^2 - 2V_{SP}V_D \cos\beta_D + V_{SP}^2 - \delta V_D^2 = 0 \tag{17}$$

$$\cos\theta_D \le +1 \Rightarrow V_D \cos\beta_D + \delta V_D - V_{SP} \ge 0 \tag{18}$$

$$\cos\theta_D \ge -1 \Rightarrow V_D \cos\beta_D - \delta V_D - V_{SP} \le 0 \tag{19}$$

Equations (17), (18) and (19) are equivalent to Eqs. (15) and (16). Transgression of Eq. (19) means the vehicle getting to the beginning of deploy stage in such state that, even with pointing opposite to the desired orbital orientation, it would not be possible to brake it sufficiently to achieve the specific velocity for the orbit. Assuming that such adverse state is physically unattainable, Eq. (19) is taken as implicitly satisfied and will not be considered hereafter.

3.2. Ascent stage end requirements

In the foregoing conditions, variables V_D and β_D refer to the starting of deploy stage. Let R_f be the geocentric distance, V_f the velocity and β_f the trajectory angle, at the end of ascent stage. As the trajectory between end of ascent stage and start of deploy stage is Keplerian, from the conservation of angular momentum and of energy, we get:

$$R_{SP}V_D \cos\beta_D = R_f V_f \cos\beta_f \tag{20}$$

$$V_D^2/2 - V_{SP}^2 = V_f^2/2 - \mu/R_f \tag{21}$$

From Eqs. (20), (21), (17) and (18), and doing convenient substitutions of variables V_f and β_f for variables V_{rf} and V_{cf}, considering that $V_{rf} = V_f \sin\beta_f$, $V_{cf} = V_f\cos\beta_f$, $V_f^2 = V_{rf}^2+V_{cf}^2$, result:

$$\Psi_1(R_f, V_{rf}, V_{cf}) = 2\omega_{SP}R_f V_{cf} + 2\mu/R_f - V_{rf}^2 - V_{cf}^2 - 3V_{SP}^2 + \delta V_D^2 = 0 \tag{22}$$

$$R_f V_{cf}/R_{SP} + \delta V_D - V_{SP} \ge 0 \tag{23}$$

where $\omega_{SP} = V_{SP}/R_{SP}$. Considering the tridimensional Cartesian space defined by coordinates R, V_r and V_c, Eq. (22) defines a surface, target set, in this space, whose points (R_f, V_{rf}, V_{cf}) satisfy the condition Ψ_1. Figure 1 illustrates a sample section of such surface, generated for a orbital radius R_{SP} = 7128 Km (altitude H_{SP} = 750 Km) and deploy stage incremental velocity δV_D = 3,47 Km/s.

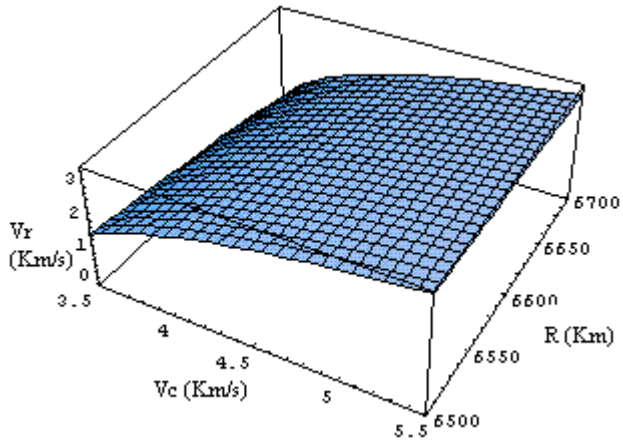

Figure 1. Target surface for the end of ascent stage (R_{SP} = 7128 Km; δV_D = 3,47 Km/s)

In the course of the ascent stage, vehicle's state variables $R(t)$, $V_r(t)$ and V_c (t) describe a phase trajectory in the above space, determined by vehicle's state equations, and with initial point settled by initial conditions R_0, V_{r0} and V_{c0}. Trajectory design is to quantify control, pitch angle $\theta(t)$, so that end point (R_f, V_{rf}, V_{cf}) of trajectory lies on target surface. To mitigate discrepancies due to occurrence of end point before or after interception of phase trajectory with target surface, such interception should be tangential, which means orthogonality between state equations vector and gradient on the surface in the set $\Psi_1(R_f, V_{rf}, V_{cf})$, that is, null scalar product between the vectors:

$$\Psi_2 = \left(dR_f/dt, dV_{rf}/dt, dV_{cf}/dt\right) \circ \left(\partial\Psi_1/\partial R_f, \partial\Psi_1/\partial V_{rf}, \partial\Psi_1/\partial V_{cf}\right) = 0 \tag{24}$$

Beyond atmosphere, active forces are thrust (consequent acceleration of magnitude a, with radial and circumferential components $a_r = a \sin\theta$ and $a_c = a \cos\theta$) and gravity (acceleration $-\mu/R^2$). Hence, state equations are:

$$dR/dt = V_r\,; \quad dV_r/dt = a\sin\theta - \mu/R^2 + V_c^2/R\,; \quad dV_c/dt = a\cos\theta - V_r V_c/R \tag{25}$$

Effectuating the scalar product in Eq. (24), we get the additional condition for the end of ascent stage:

$$\Psi_2(R_f, V_{rf}, V_{cf}, \theta_f) = V_{rf}\tan\theta_f + V_{cf} - \omega_{SP} R_f = 0 \tag{26}$$

3.3. Ascent trajectory problem formulation

The state variables for this model are geocentric distance $R(t)$, radial velocity $V_r(t)$, circumferential velocity V_c (t) and pitch angle $\theta(t)$, all local but geo-inertially referred. Thrust acceleration of magnitude a, with its radial and circumferential components a_r and a_c , is also time-variable. However, it is not necessary taking it as a formal state variable, because its variation is modeled through a linear approximation of predicted thrust and mass outflow, so that its values at any instant of ascent stage may be directly calculated, independently of integration. The angular velocity $\omega_a(t)$, temporal variation of $\theta(t)$, is the formal control variable for the model. From Eqs. (25), state equations are:

$$\dot{\mathbf{x}} = \left(\dot{R} \quad \dot{V}_r \quad \dot{V}_c \quad \dot{\theta}\right)^T = \begin{pmatrix} V_r \\ a\sin\theta - \mu/R^2 + V_c^2/R \\ a\cos\theta - V_r V_c/R \\ \omega_a \end{pmatrix} \tag{27}$$

From Eqs. (22) and (26), the equality final conditions are given by:

$$\boldsymbol{\Psi} = \begin{pmatrix} \Psi_1 \\ \Psi_2 \end{pmatrix} = \begin{pmatrix} 2\omega_{SP} R_f V_{cf} + 2\mu/R_f - V_{rf}^2 - V_{cf}^2 - 3V_{SP}^2 + \delta V_D^2 \\ V_{rf}\tan\theta_f + V_{cf} - \omega_{SP} R_f \end{pmatrix} = \begin{pmatrix} 0 \\ 0 \end{pmatrix} \tag{28}$$

Performance index is conveniently chosen and its minimization is set as criterion for solution:

$$PI = -K_m R_f V_{cf} + K_\omega \int_{t_0}^{t_f} \left(\omega_a^2/2\right) dt \tag{29}$$

where K_m and K_ω are positive weighting parameters. Stressing the increase of the product $R_f V_{cf}$, we stress the fulfillment of inequality final condition in Eq. (23). The integral component in the performance index is a choice aiming energy consumption reduction and also to improve convergence capability. As set forth in subsection 2.2, we define the auxiliary state variable I_ω, resulting in the following reformulated sets of state equations and initial conditions:

$$\dot{\bar{\mathbf{x}}} = \begin{pmatrix} \dot{R} & \dot{V}_r & \dot{V}_c & \dot{\theta} & \dot{I}_\omega \end{pmatrix}^T = \begin{pmatrix} V_r \\ a\sin\theta - \mu/R^2 + V_c^2/R \\ a\cos\theta - V_r V_c/R \\ \omega_a \\ \omega_a^2/2 \end{pmatrix} \tag{30}$$

$$\bar{\mathbf{x}}(t_0) = \begin{pmatrix} R_0 & V_{r0} & V_{c0} & \theta_0 & 0 \end{pmatrix}^T \tag{31}$$

We also incorporate the equality final conditions, Eq. (28), into the performance index, Eq. (29), which finally becomes:

$$\Phi = -K_m R_f V_{cf} + K_\omega I_\omega + (K_{\Psi 1}/2)\Psi_1^2 + (K_{\Psi 2}/2)\Psi_2^2 \tag{32}$$

where $K_{\Psi 1}$ and $K_{\Psi 2}$ are positive weighting parameters. Thus, we have the optimal control problem of determining a control $\omega_a(t)$ and corresponding trajectory, from t_0 to t_f, with dynamics expressed in Eq. (30), initial conditions in Eq. (31), and the performance index in Eq. (32).

3.4. Ascent trajectory problem solution with gradient method

Using Eq. (30) and introducing the adjoint vector $\bar{\boldsymbol{\lambda}}$, the Hamiltonian function H is formed:

$$H(\bar{\boldsymbol{\lambda}}, \bar{\mathbf{x}}, \omega_a) = \lambda_1 V_r + \lambda_2 \left(a\sin\theta - \mu/R^2 + V_c^2/R\right) + \lambda_3 (a\cos\theta - V_r V_c/R) + \lambda_4 \omega_a - \lambda_5 \omega_a^2/2 \tag{33}$$

The adjoint differential equations and final transversality conditions are, respectively:

$$\dot{\bar{\boldsymbol{\lambda}}} = \begin{pmatrix} \dot{\lambda}_1 & \dot{\lambda}_2 & \dot{\lambda}_3 & \dot{\lambda}_4 & \dot{\lambda}_5 \end{pmatrix}^T = -H_{\bar{\mathbf{x}}}^T = \begin{pmatrix} V_c(\lambda_2 V_c - \lambda_3 V_r)/R^2 - 2\mu\lambda_2/R^3 \\ -\lambda_1 + \lambda_3 V_c/R \\ (-2\lambda_2 V_c + \lambda_3 V_r)/R \\ a(\lambda_3 \sin\theta - \lambda_2 \cos\theta) \\ 0 \end{pmatrix} \tag{34}$$

$$\bar{\boldsymbol{\lambda}}(t_f) = -\Phi_{\bar{\mathbf{x}}(t_f)}^T = K_m \begin{pmatrix} V_{cf} \\ 0 \\ R_f \\ 0 \\ 0 \end{pmatrix} - K_\omega \begin{pmatrix} 0 \\ 0 \\ 0 \\ 0 \\ 1 \end{pmatrix} - K_{\Psi 1}\Psi_1 \begin{pmatrix} \Psi_{1R_f} \\ \Psi_{1Vr_f} \\ \Psi_{1Vc_f} \\ 0 \\ 0 \end{pmatrix} - K_{\Psi 2}\Psi_2 \begin{pmatrix} \Psi_{2R_f} \\ \Psi_{2Vr_f} \\ \Psi_{2Vc_f} \\ \Psi_{2\theta_f} \\ 0 \end{pmatrix} \tag{35}$$

where the partial derivatives of Ψ_1 and Ψ_2 are:

$$\Psi_{\bar{\mathbf{x}}} = \begin{pmatrix} \Psi_{1\bar{\mathbf{x}}} \\ \Psi_{2\bar{\mathbf{x}}} \end{pmatrix} = \begin{pmatrix} 2(\omega_{SP} V_{cf} - \mu/R_f^2) & -2V_{rf} & 2(\omega_{SP} R_f - V_{cf}) & 0 & 0 \\ -\omega_{SP} & \tan\theta_f & 1 & V_{rf}/(\cos\theta_f)^2 & 0 \end{pmatrix}$$

The partial derivative of the Hamiltonian H with respect to ω_a, and the iterative control adjustment $\delta\omega_a$ are:

$$H_{\omega_a} = \lambda_4 + \lambda_5 \omega_a \tag{36}$$

$$\delta\omega_a = K \left(\int_{t_0}^{t_f} H_{\omega_a}^2 \, dt \right)^{-1/2} H_{\omega_a} \tag{37}$$

Thus, the general procedure described at the end of subsection 2.3 may be applied to find a solution to this ascent trajectory design problem.

3.5. Control law after target attaining instant

As approached in subsection 3.2, the target attaining instant is that at which phase trajectory should intercept target surface. Even with Eq. (26) directing this interception to be tangential, depending on the amount of eventual remaining burning propellant, continuing phase trajectory might get significantly away from target surface, with corresponding change in the attainable orbital radius. To avoid this, we impose the continuing phase trajectory to keep adherent to the target surface. To keep Eq. (26) holding at any point, we get from Ψ_2 the following reference pitch angle, as a function of ongoing $R(t)$, $V_r(t)$, $V_c(t)$, which is to drive trajectory after target attaining instant:

$$\theta = \arctan\left((\omega_{SP} R - V_c)/V_r\right) \tag{38}$$

4. SIMULATIONS

Simulation cases have been performed with a software prototype, built for assessment tests of the trajectory design model. The prototype runs concurrently with another available software which simulates a target launch vehicle. Results from a mission case with designed orbit altitude H_{SP} = 750 Km are presented here. To confront these results with those obtained from the same mission case, but running the trajectory design software as described in (Nepomuceno, 2006), which is an application of neighboring extremals method, each figure here shows plotted results from both.

In simulation tests, we may consider attainable circular orbit radius as a variable R_S, corresponding to an altitude H_S, with value to be determined by the values of the other variables – R_f, V_{rf}, V_{cf}, at the end of stage. This way, we consider Eq. (22) as a third-degree equation on variable $\sqrt{R_S}$. Within the mathematical solutions to the equation, one has physical meaning for our case, and it has been used to plot the attainable circular orbit altitude H_S along the ending course of the stage. Moreover, from Eqs. (15) and (20), with $V_f \cos\beta_f = V_{cf}$, we also plot the predicted pointing angle θ_D along the ending course of the ascent stage, as determined by the values of other variables, including the above R_S.

4.1. Designed trajectories

The outputs presented here refer to the designed trajectory without any "in-flight" feedback along the own trajectory, that is, produced only with the available data at the beginning of the trajectory. Figure 2 shows the designed evolution of the formal control variable. Figure 3 shows the state variables designed evolution. The outlines of what should be the attainable circular orbit altitude and associated predicted pointing angle, as if burnout suddenly occurs at the corresponding instant in the designed trajectory, are shown in Fig. 4.

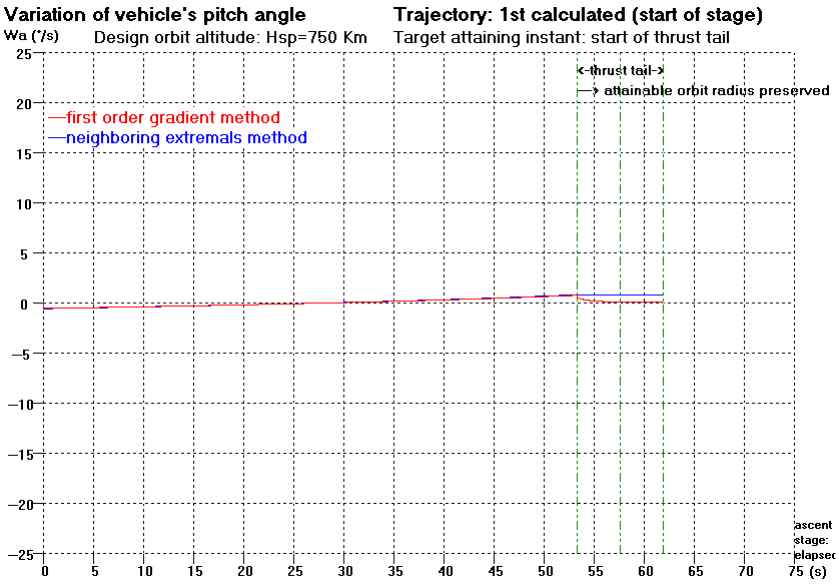

Figure 2. Control evolution in designed trajectory

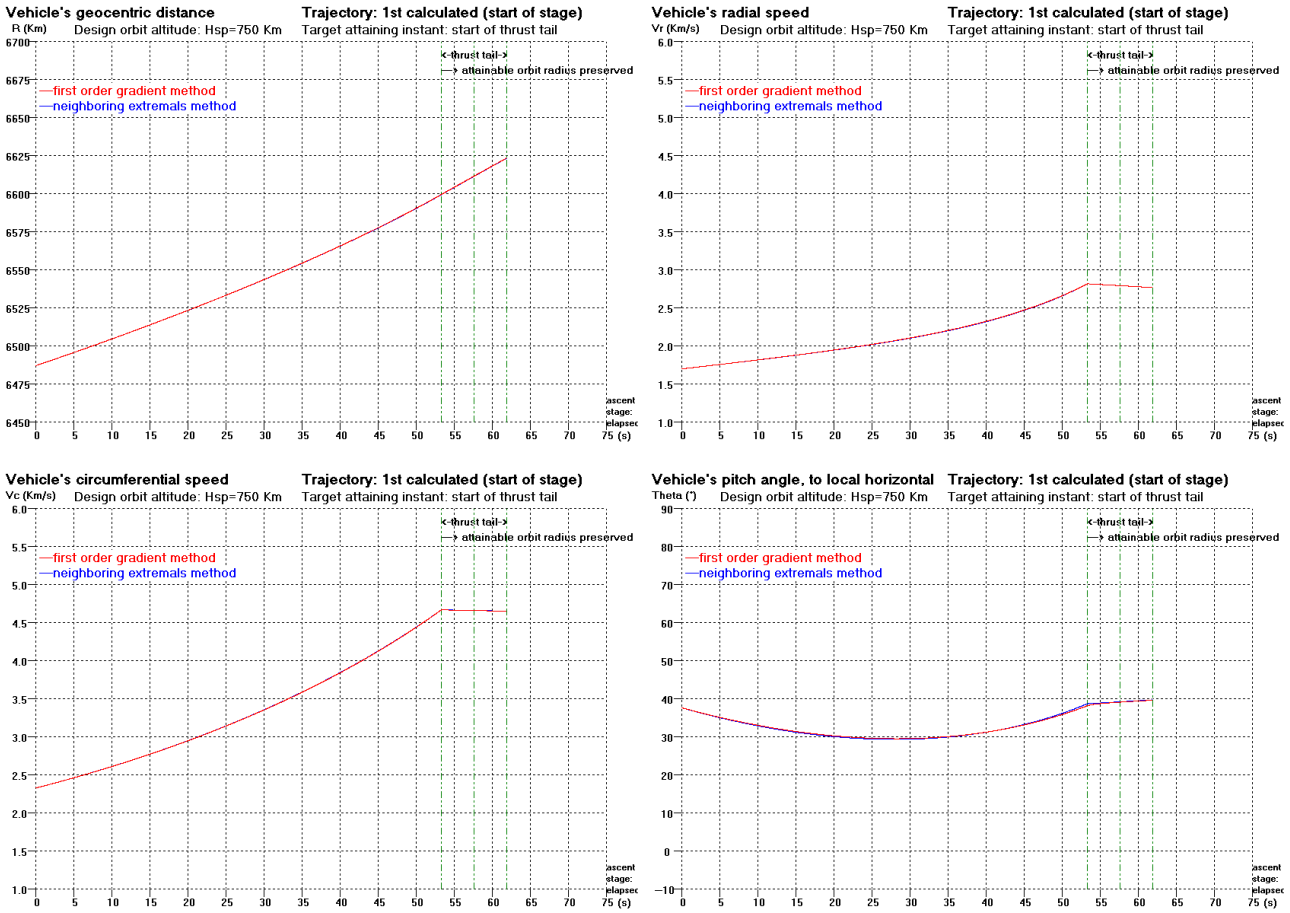

Figure 3. State evolution in designed trajectory

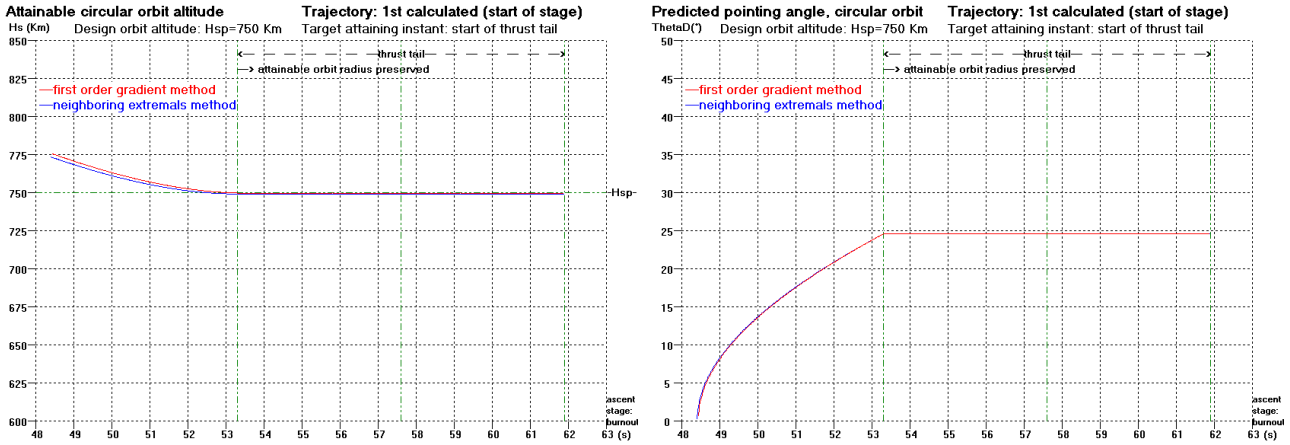

Figure 4. Designed trajectory: attainable circular orbit altitude and predicted pointing angle

We verify in Fig. 4 that the attainable circular orbit altitude $H_S(t)$ assumes the designed value H_{SP} at the target attaining instant (due to condition Ψ_1, Eq. (22)); at this instant the curve $H_S(t)$ intercepts tangentially the horizontal line $H_S=H_{SP}$ (due to condition Ψ_2, Eq. (26)); and after that, $H_S(t)$ remains with the value H_{SP} (due to control law Eq. (38)). The time instant corresponding to initial point of outlined curve for attainable altitude $H_S(t)$, as for predicted pointing angle $\theta_D(t)$, is the starting instant it is achieved feasibility of later circular orbit injection, if burnout suddenly occurs.

4.2. Guided trajectories

The outputs presented here refer to the guided trajectory as performed by the launch vehicle simulator, interacting with the prototype for the trajectory design model, which fulfills a guidance task. Figure 5 shows the performed evolution of the formal control variable. Figure 6 shows the state variables performed evolution. The outlines of what

should be the attainable circular orbit altitude and associated predicted pointing angle, as if burnout suddenly occurs at the corresponding instant in the performed trajectory, are in Fig. 7.

With respect to Fig. (7), refer to what have been pointed out for Fig. (4), within designed trajectories in foregoing subsection, here applied to guided trajectories.

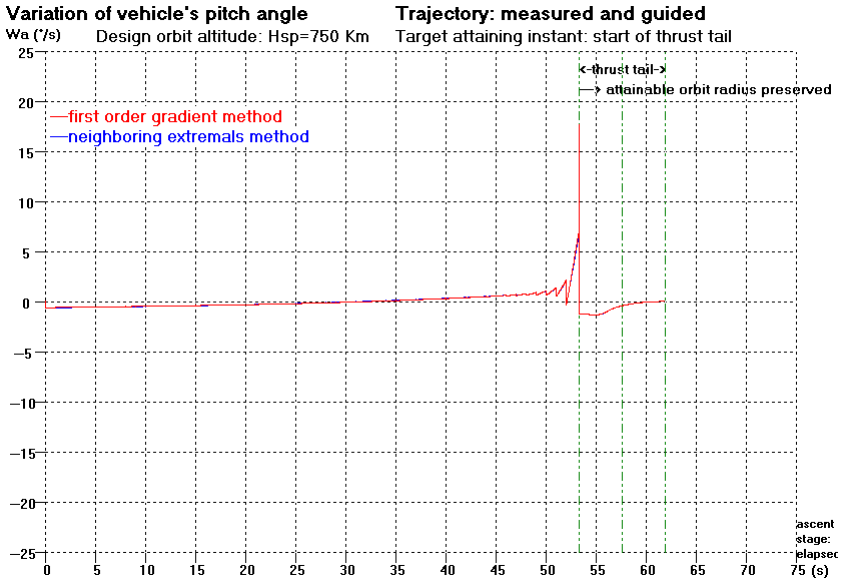

Figure 5. Control evolution in guided trajectory

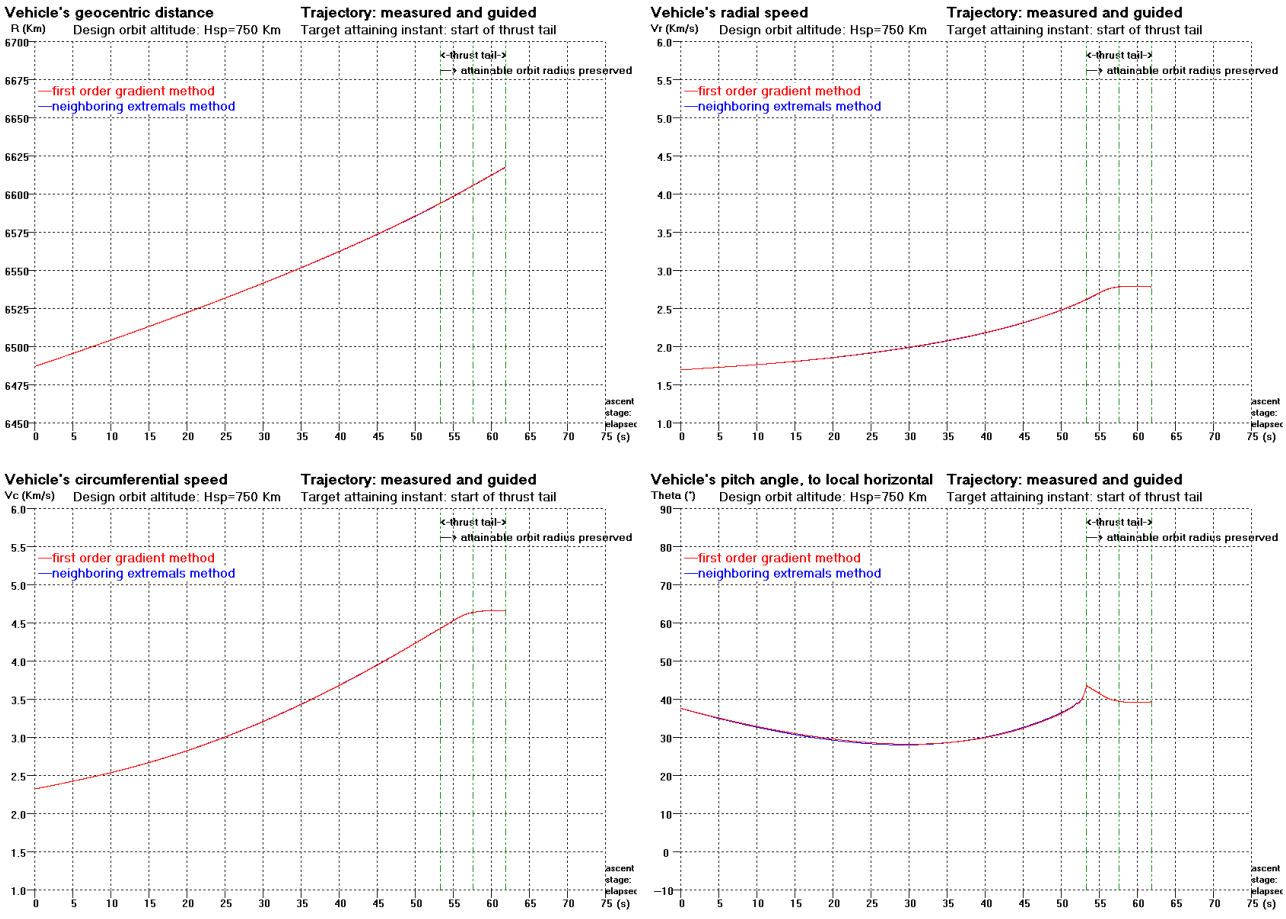

Figure 6. State evolution in guided trajectory

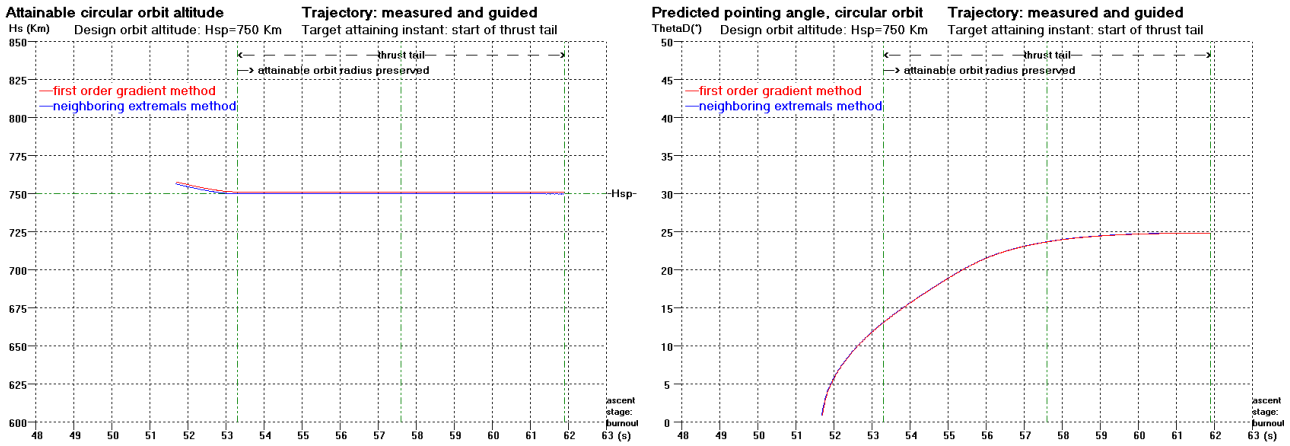

Figure 7. Guided trajectory: attainable circular orbit altitude and predicted pointing angle

5. CONCLUSION

Trajectory design and related optimization issues may be performed by means of many available techniques, especially for the numerical solving. It is usual to classify the solution methods as either direct or indirect; and what we have presented here uses a technique, first order gradient, classified as a direct method. Results from a simulation test have been shown along with the results from another test for the same mission case, but running a trajectory design software applying the neighboring extremals technique, classified as indirect method. We observe that the resulting optimal solutions are very similar to each other, despite precision criteria are not the same. Simulation tests have shown good results, although we have met some difficulties, with the gradient method, in tuning the weighting parameters and the step in control corrections; whereas initial setting of values for adjoint variables and convergence had represented main difficulties with the neighboring extremals method. These are issues for continuing research.

6. REFERENCES

Bryson Jr., Arthur E.; Ho, Yu-Chi, 1975, "Applied Optimal Control: Optimization, Estimation and Control", Washington, DC, Hemisphere.

Golfetto, Wander A, 2004, "Aplicações de Métodos de Segunda Ordem para a Otimização de Trajetórias Espaciais", 270 f, Tese (Doutorado em Ciências), Instituto Tecnológico de Aeronáutica, São José dos Campos.

Leite Filho, Waldemar C.; Pinto, Pelson S., 1998, "Guidance Strategy for Solid Propelled Launchers", Journal of Guidance, Control, and Dynamics, v. 21, n. 6, pp. 1006-1009.

McIntyre, John E, 1968, "Guidance, Flight Mechanics and Trajectory Optimization: the Pontryagin Maximum Principle", v. VII. Downey, NASA (NASA CR-1006).

Nepomuceno, Abel L., 2006, "Guiamento do VLS-1 com Prevenção para Dispersões em Parâmetros Pré-Estabelecidos", 202 f, Dissertação (Mestrado em Engenharia Aeroespacial), Instituto Tecnológico de Aeronáutica, São José dos Campos.

7. RESPONSIBILITY NOTICE

The authors are the only responsible for the printed material included in this paper.